A novel Schiff base: synthesis, structural characterisation and comparative sensor studies for metal ion detections

Muhammet Kose, Savas Purtas, Seyit Ali Gungor, Gokhan Ceyhan, Eyup Akgun, Vickie McKee

PII: S1386-1425(14)01522-4
DOI: http://dx.doi.org/10.1016/j.saa.2014.10.025
Reference: SAA 12840

To appear in: *Spectrochimica Acta Part A: Molecular and Biomolecular Spectroscopy*

Received Date: 12 February 2014
Revised Date: 8 October 2014
Accepted Date: 9 October 2014

Please cite this article as: M. Kose, S. Purtas, S.A. Gungor, G. Ceyhan, E. Akgun, V. McKee, A novel Schiff base: synthesis, structural characterisation and comparative sensor studies for metal ion detections, *Spectrochimica Acta Part A: Molecular and Biomolecular Spectroscopy* (2014), doi: http://dx.doi.org/10.1016/j.saa.2014.10.025

A novel Schiff base: synthesis, structural characterisation and comparative sensor studies for metal ion detections

Muhammet Kose[1], Savas Purtas[1], Seyit Ali Gungor[1], Gokhan Ceyhan[1], Eyup Akgun[1], Vickie McKee[2]

[1]*Department of Chemistry, Kahramanmaraş Sütçü Imam University, Kahmaranmaraş, 46050, Turkey*

[2]*Department of Chemistry, Loughborough University, Leicestershire, LE11 3TU, UK*

Corresponding author: Muhammet Kose

Tel.: +90 344 280 1408

Fax: +90 344 280 1352

E-mail address: *muhammetkose@ksu.edu.tr*

Abstract

A novel Schiff base ligand was synthesized by the condensation reaction of 2,6-diformylpyridine and 4-aminoantipyrine in MeOH and characterized by its melting point, elemental analysis, FT-IR, ^{1}H-, ^{13}C-NMR and mass spectroscopic studies. Molecular structure of the ligand was determined by single crystal X-ray diffraction technique. The electrochemical properties of the Schiff base ligand were studied in different solvents at various scan rates. Sensor ability of the Schiff base ligand was investigated by colorimetric and fluorometric methods. Visual colour change of the ligand was investigated in MeOH solvent in presence of various metal ions Na^{+}, Mg^{2+}, Al^{3+}, K^{+}, Cr^{3+}, Mn^{2+}, Fe^{3+}, Co^{2+}, Ni^{2+}, Cu^{2+}, Zn^{2+}, Cd^{2+}, Hg^{2+} and Pb^{2+}. Upon addition of Al^{3+} ion into a MeOH solution of the ligand, an orange colour developed which is detectable by naked eye. Fluorescence emission studies showed that the ligand showed single emission band at 630-665 nm upon excitation at 560 nm. Addition of metal ions Na^{+}, Mg^{2+}, K^{+}, Cr^{3+}, Mn^{2+}, Fe^{3+}, Co^{2+}, Ni^{2+}, Cu^{2+}, Zn^{2+}, Cd^{2+}, Hg^{2+} and Pb^{2+} (1:1 molar ratio) cause fluorescence quenching, however addition of Al^{+3} resulted in an increase in fluorescence intensity. No significant variation was observed in the fluorescence intensity caused by Al^{3+} in presence of other metal ions. Therefore, the Schiff base ligand can be used for selective detection of Al^{3+} ions in the presence of other metal ions the other metal ions studied.

Keywords: Schiff base, Structural characterisation, Visual detection, Colorimetric and Fluorometric sensor.

1 Introduction

There are several analytical methods such as atomic absorption spectrometry [1], inductively coupled plasma emission spectrometry [2, 3], gravimetric [4, 5], chromatography [6, 7], anodic stripping voltammetry [8, 9] and ion selective electrodes [10-11] proposed for detection of metal ions. These methods demand relatively high cost apparatus, involving multi-step sample pre-treatments [12]. Therefore, selective detection of metal ions by colourimetric or fluorescent chemosensors has received a particular attention [13]. Among these, the selective detection of transition metal ions has gained special attention due to their crucial role in biological and environmental processes [14-16].

Schiff base condensations yield compounds with wide uses as ligands [17, 18]. Schiff bases are reported to possess several biological activities such as antimicrobial [19], antifungal [20], anticancer [21] and cytotoxic [22] activities. There are numerous papers published on transition metal complexes of Schiff bases on regarding their antimicrobial activity [23] thermal studies [24], electrochemical properties [25], as electrochemical sensors [26], and as catalysts for epoxidation of olefins, lactide polymerization, ring opening of epoxides and Michael reactions [27]. Recently, a number of Schiff base compounds have been used as colorimetric sensors [28-30]. Schiff bases can form coordination bonds with many metal ions through phenolic and azomethine groups. Therefore, Schiff bases can recognise the metals *via* these binding sites, because of this reason they are used to design a chemosensor as sensing materials.

In this paper, a novel Schiff base ligand (L) was synthesised by the reaction of one equivalent 2,6-diformylpyridine with two equivalents of 4-aminoantipyrine (Scheme 1). The ligand was characterised by FT-IR, ^{1}H-, ^{13}C-NMR and mass spectroscopic studies. Molecular structure of the ligand was determined by single crystal X-ray diffraction study. Sensor ability of the Schiff base ligand to colorimetrically sense metal ions Na^{+}, Mg^{2+}, Al^{3+}, K^{+}, Cr^{3+}, Mn^{2+}, Fe^{3+}, Co^{2+}, Ni^{2+}, Cu^{2+}, Zn^{2+}, Cd^{2+}, Hg^{2+} and Pb^{2+} was investigated.

2 Experimental

2.1 Materials

All starting materials and organic solvents were purchased from commercial sources and used as received unless otherwise noted. The solutions of metal ions were prepared from their chloride or nitrate salts.

2.2 Physical Measurements

FT-IR spectrum of the ligand was performed using KBr pellets on a Perkin Elmer Paragon 1000PC. CHN analysis was performed using a LECO CHNS 932. The ^{1}H and ^{13}C NMR spectra were performed on a Bruker Avance 500. ESI mass spectrum was recorded on a LC/MS APCI AGILENT 1100 MSD spectrophotometer. The electronic spectra in the 200–900 nm range were obtained on a Shimadzu UV-1800 UV-Vis spectrophotometer. The single-photon fluorescence spectra were collected on a Perkin Elmer LS55 luminescence spectrometer.

Data collection for X-ray crystallography was completed using a Bruker APEX2 CCD diffractometer and data reduction was performed using Bruker SAINT. SHELXTL was used to solve and refine the structures [31].

Stock solutions of the Schiff base ligand (L) were prepared in DMF ($1x10^{-4}$ M) for electrochemical studies. All voltammetric measurements at the glassy carbon electrode were performed using a BAS 100W (Bioanalytical System, USA) electrochemical analyser. A glassy carbon working electrode (BAS; Φ: 3mm diameter), an Ag/AgCl reference electrode (BAS; 3M KCl) and platinum wire counter electrode and a standard one-compartment three electrode cell of 10 mL capacity were used in all experiments. The glassy carbon electrode was polished manually with aqueous slurry of alumina powder (*Φ*: 0.01 μm) on a damp smooth polishing cloth (BAS velvet polishing pad), before each measurement. All measurements were performed at room temperature. Mettler Toledo MP 220 pH meter was used for the pH measurements using a combined electrode (glass electrode reference electrode) with an accuracy of ± 0.05 pH.

2.3 Preparation of the ligand

The ligand was synthesized from the simple reaction of one equivalent of 2,6-diformylpyridine and two equivalents of 4-aminoantipyrine in MeOH. A solution of 4-aminoantipyrine (1.02 g, 5 mmol) in MeOH (15ml) was added dropwise to a MeOH solution (30ml) of 2,6-diformylpyridine (0.38 g, 2.5 mmol). A pale yellow colour appeared and a precipitate formed in a few minutes. The reaction mixture was stirred for two hours, and then the yellow product was collected by filtration, washed with diethyl ether and dried in air.

Yield: 1.18 g, 94%, m.p 118-122 ºC. CHN Analysis Calc. for $C_{29}H_{27}N_7O_2$: C, 68.28; H, 5.39; N, 19.40%. Found: C, 68.12; H, 5.35; N, 19.37%. ESI-MS (m/z (rel. intensity) assignment): 506(100%) $[M+H]^+$, 528(50%) $[M+Na]^+$. ^{1}H-NMR ($CDCl_3$ as solvent, δ in ppm):2.52 (*s,* 6H,

C-CH_3), 3.18 (*s*, 6H, C-CH_3), 7.33 (*t,* 2H, CH benzene), 7.39(*d,* 4H, CH benzene), 7.50 (*t,* 4H, CH benzene), 7.81(*t,* 1H, CH pyridine, 7.99 (*d,* 2H, pyridine), 9.81 (s, CH=N).^{13}C NMR ($CDCl_3$ as solvent, γ in ppm): 10.26 (CH_3), 35.57 (NCH_3), 118.15-156.73 (C, aromatic), 160.31 (C, C=N). IR (KBr disk cm^{-1}): 2923, 2853, 1645, 1581, 1491, 1443, 1408, 1375, 1302, 1136, 1076, 1026, 953, 823, 767, 701, 624.

2.4 X-ray Structure Solution and Refinement

A single crystal of dimensions 0.47 x 0.42 x 0.22 mm^3 was chosen for the diffraction experiment. Data were collected at 150(2)K on a Bruker ApexII CCD diffractometer using Mo-*Kα* radiation(λ = 0.71073Å). The structure was solved by direct methods and refined on F^2 using all the reflections [32]. All the non-hydrogen atoms were refined using anisotropic atomic displacement parameters and hydrogen atoms bonded to carbon atoms were inserted at calculated positions using a riding model. Details of the crystal data and refinement are given Table 1. Hydrogen bond parameters are given in Table 2 and selected bond lengths are given in Table 3.

3 Results and Discussion

3.1 Characterization of the ligand

2,6-Diformylpyridine was prepared by oxidation of 2,6-pyridinedimethanol according to the reported method [33]. The ligand (L) was prepared by a Schiff base condensation reaction of one equivalent of 2,6-diformylpyridine and two equivalents of 4-aminoantipyrine with high yield and purity (Scheme 1). The pale yellow product is stable at room temperature in the solid state without decomposition and soluble in common organic solvents such as MeOH, ethanol, acetonitrile, chloroform, dichloromethane, DMF and DMSO. The molecule has two azomethine groups and two antipyrine units each side of pyridine. Elemental analysis results are given in the experimental section and are in good agreement with the calculated values.

The ^{1}H- and ^{13}C-NMR spectra were recorded in $CDCl_3$, and the spectral data are given in the experimental section. The ^{1}H and ^{13}C NMR spectra of the ligand are given in Figs. S1&2. The ligand shows mirror symmetry in $CDCl_3$ solution. The ^{1}H-NMR spectrum of the ligand displays two singlets at δ 2.52 and 3.18 ppm corresponding to protons of two methyl groups (C-CH_3 and N-CH_3, respectively), a singlet at δ 9.81 ppm assigned to azomethine protons

(–N=CH-) [34]. A dublet at δ 7.99 ppm and a triplet at δ7.81 ppm in 2:1 ratio were assigned to the pyridine protons. Two triplets at δ 7.33 and 7.50 and a dublet at δ 7.39 in 1:2:2 ratios were assigned to the benzene protons. The ^{13}C NMR spectrum of the ligand exhibited the signals due to the presence of aromatic and methyl carbons. Two methyl carbon shifts were seen at δ 20.81 ppm. The signal at δ 156.08 ppm could be assigned to azomethine carbons (-N=C-) [34]. All the other aromatic carbon shifts were observed in the range of δ 115.21 – 154.50 ppm.

The ESI mass spectrum of the ligand is recorded in MeOH and depicted in Fig. S3. In the ESI mass spectrum of the ligand two signals at m/z 506(100%) and 528(50%) were assigned to molecular ion peaks $[M+H]^+$ and $[M+Na]^+$, respectively.

In the IR spectrum of the ligand, the bands observed at 2923 and 2853 cm^{-1} can be attributed to the aliphatic $\nu_{(C-H)}$ vibrations. The carbonyl $\nu_{(C=O)}$ and azomethine $\nu_{(CH=N)}$ vibrations were observed at 1645 and 1581 cm^{-1}, respectively [35].

3.2 Crystal structure of the ligand

Single crystals for X-ray diffraction study were obtained by slow evaporation of a THF solution of the ligand. Perspective view of the ligand is shown in Fig. 1. The ligand crystallizes in monoclinic crystal system, $P2_1/n$ space group with unit cell parameters a = 9.3088(17), b = 21.050(4), c = 13.575(2) Å, β = 101.424(3)°, V = 2607.2(8) $Å^3$ and Z = 4. The molecule has no crystallographically imposed symmetry. All bond lengths and angles are within the normal ranges. The molecule has two azomethine groups and two antipyrine unit each side of the pyridine ring. The azomethine linkage distances are 1.2805(17) and 1.2776(18) Å for N3-C12 and N5-C18 and within the range of normal C=N values [36]. The C7-O1 and C19-O2 bond distances are 1.2362(17) and 1.2354(17) Å, respectively [36]. The C8-C9 and C20-C21 bond distances shows C-C double bond character with distances of 1.377(2) and 1.362(2) Å, respectively.

In the structure, both five membered antipyrine rings (N1-C7-C8-C9-N2 and N6-C19-C20-C21-N7) slightly twisted with respect to the central pyridine ring. The mean planes of N1-C7-C8-C9-N2 and N6-C19-C20-C21-N7 are at 1.89(8) and 8.86(8)° to the central (C13-N4) ring, respectively. Outer benzene rings (C1-C6 and C24/C29) significantly twisted with respect to the central pyridine ring. Dihedral angle between the outer benzene rings and pyridine ring are 70.45(5) and 51.47(5)° for C1-C6/C13-N4 and C24-C29/C13-N4, respectively. This is possibly a consequence of the intermolecular interactions in the lattice.

There are two sets of π...π edge-edge stacking interactions in the ligand (Fig. 2). First, C18-O2 section of the ligand is stacked with the same section of an adjacent molecule; C18 and O2 are separated by 3.301Å (symmetry operation: 1-x, -y, 1-z). Second, C4-C5 edge of benzene ring is stacked with the same section of a neighbouring molecule under symmetry operation of 1-x, 1-y, 1-z; C4 and C5 are separated by 3.455Å.

In the crystal structure of the ligand, molecules are linked *via* weak hydrogen bond type interactions (CH·····N and CH·····O). The same hydrogen bond contacts are extended between the other symmetry-related molecules in their respective planes to form hydrogen bonding network (Fig. 3& Table 2).

3.3 Electrochemical properties of the ligand

Electrochemical properties of the ligand were investigated in DMF -0.1 M NBu_4BF_4 as supporting electrolyte at 293 K. In order to study the effects of the solution concentration and the scan rates, two different concentrations and the scan rates were used (in the 100-1000 mV/s range) and against an internal ferrocence-ferrocenium standard [37]. The electrochemical data are given in Table 4. The electrochemical curves of Schiff base ligand is shown in Fig. S4. The ligand in the 1×10^{-3} M and 100-1000 mv/s range shows the three anodic peak potentials in the -0.43-1,74 V range. In this scan rate range, the ligand shows three cathodic peak potentials in the -1.42 - 1.14 V range. Similarly, in the 1×10^{-4} M and 100-1000 mv/s range show the three anodic peak potentials in the -0.66 - 1.56 V range. In this scan rate range, the ligand shows three cathodic peak potentials in the 1.38 – 1.52 V range.
In 1×10^{-3} M concentration, the ligand shows the reversible process (I_{pa}: I_{pc}= 1.02) at the 500 and 750 mVs^{-1} scan rates. Their potential ranges change from 0.41 V to -1.34 V (E_{pc}) and -0.41 V to 1.7 V (E_{pa}). At the other scan rate, the ligand shows the irreversible process (I_{pa}: $I_{pc}\neq$ 1.0) at the 1.14 V (E_{pc}) and -0.43 V (E_{pa}). All the oxidation and reduction processes of the ligand 1×10^{-4} M DMF solutions at the100-1000mV/s scan rates are irreversible. These processes are shown are in Fig. S5.

3.4 Visual colour change

Visual colour change of the ligand (0.1mM) was investigated in MeOH solvent in presence of various metal ions Na^+, Mg^{2+}, Al^{3+}, K^+, Cr^{3+}, Mn^{2+}, Fe^{3+}, Co^{2+},Ni^{2+}, Cu^{2+}, Zn^{2+}, Cd^{2+}, Hg^{2+} and Pb^{2+} (0.1 mM) in 1:1 molar ratio (Fig. 4). The ligand is colourless in MeOH solution. Addition of Na^+, Mg^{2+} and K^+ caused no colour change. However, upon addition of

Al^{3+} ion into the MeOH solution of the ligand, an orange colour developed which is detectable by naked eye. Under similar condition, Cr^{3+}, Fe^{3+}, Cu^{2+} ions produce pale pink colour. Other ions such as Mn^{2+}, Co^{2+}, Ni^{2+}, Zn^{2+}, Cd^{2+}, $Hg^{2+}$and Pb^{2+} exhibit light yellow to yellow colour, which is difficult to distinguish from one another by naked eye.

3.5 UV-vis spectral studies

The chemosensor behaviour of the Schiff base ligand (0.1mM) was investigated by monitoring the UV–vis absorption spectral behaviour upon addition of various metal ions Na^{+}, Mg^{2+}, Al^{3+}, K^{+}, Cr^{3+}, Mn^{2+}, Fe^{3+}, Co^{2+}, Ni^{2+}, Cu^{2+}, Zn^{2+}, Cd^{2+}, Hg^{2+} and Pb^{2+} in 1:1 molar ratio in MeOH. The UV–vis spectrum of free ligand shows two absorption bands at 230 and 352 nm. The band at 230 nm could be due to π–π* transition and second band at 352 nm could be assigned to transition of n–π* in Schiff base moiety.

Upon the addition of metal ions Al^{3+}, K^{+}, Cr^{3+}, Mn^{2+}, Fe^{3+}, Co^{2+}, Ni^{2+}, Cu^{2+}, Zn^{2+}, Cd^{2+}, Hg^{2+} and Pb^{2+} (0.1mM) in 1:1 molar ratio in MeOH, a new absorption peak appeared at region of 400–550 nm (Fig. 5) showing complexation between the Schiff base ligand and metal ion. The strongest absorption peak was observed when Al^{3+} ion was used with ligand over other sensed ions. The absorption bands of the Schiff base also shifted to lower absorption values indicating the involvement of imine and carbonyl oxygen atoms in coordination with metal ion. Addition of Na^{+}, Mg^{2+}, Al^{3+} and K^{+} (0.1 mM) in MeOH, the absorption bands of the Schiff base ligand shifted lower intensity, however no new absorption band was observed.

To gain insight into the stoichiometry of the ligand-metal complex, the method of continuous variations (Job's plot) was used [38]. In this method, the total concentration (0.1 mM) and volume (10 mL) of ligand and Al^{3+} ion were kept constant, and changing the molar ratio of the ligand from 0.0 to 1.0. The results show that when the molar ratio of ligand is 0.5, ligand-metal ion complex absorbance value reaches a maximum indicating that forming a 1:1 ligand-metal ion ratio (Fig. 6). The possible coordination mode of the ligand and Al^{3+} is shown in Fig. 7. In the complex, the metal ion possibly binds to the pyridine diimine unit and oxygen atoms of antipyrine moiety.

UV–vis spectrophotometric titrations were performed to understand the interaction between the ligand (L) and Al^{3+} ion. The plot of UV–vis absorption intensity versus concentration indicated that the intensities of the colorimetric sensor L were proportional to the Al^{3+} concentration. The intensity plot of L versus Al^{3+} concentration at 448 nm exhibited

a linear response (r^2 = 0.998) from 1 μM to 10 μM. Clear isosbestic points were observed at 395 nm, indicating the formation of L-Al^{3+} complex (Fig. 8).

3.6 Fluorescence emission studies

Fluorescence emission studies were performed to investigate the selectivity of the ligand towards various metal ions Na^+, Mg^{2+}, Al^{3+}, K^+, Cr^{3+}, Mn^{2+}, Fe^{3+}, Co^{2+}, Ni^{2+}, Cu^{2+}, Zn^{2+}, Cd^{2+}, Hg^{2+} and Pb^{2+}in MeOH. Fluorescence spectra of the ligand showed single emission band at 630-665 nm upon excitation at 560 nm. Addition of metal ions Na^+, Mg^{2+}, K^+, Cr^{3+}, Mn^{2+}, Fe^{3+}, Co^{2+}, Ni^{2+}, Cu^{2+}, Zn^{2+}, Cd^{2+}, Hg^{2+} and Pb^{2+} (1:1 molar ratio) cause fluorescence quenching. Quenching of fluorescence intensity of the ligand by metal ions during complexation can be explained by processes such as redox-activity, magnetic perturbation and electronic energy transfer, *etc.* [39]. However, addition of Al^{+3} resulted in an increase in fluorescence intensity (Figs. 9&10). The addition of Al^{3+} causes an enhancement in the fluorescence intensity in a concentration dependent manner. Upon addition of Al^{3+}, an immediate response occurs and the maximum fluorescence intensity has been observed on addition of an equivalent of Al^{3+} in MeOH solution of the ligand (0.1mM) (Fig. 11). The selectivity of the ligand for sensing Al^{3+} ions was determined by performing competitive experiments of the Al^{3+} solutions mixed with other common interfering metal ions Na^+, Mg^{2+}, K^+, Cr^{3+}, Mn^{2+}, Fe^{3+}, Co^{2+}, Ni^{2+}, Cu^{2+}, Zn^{2+}, Cd^{2+}, Hg^{2+} and Pb^{2+}. No significant variation was observed in the fluorescence intensity caused by Al^{3+} in presence of other metal ions. Thus, the Schiff base ligand can be used for selective sensor for detection of Al^{3+} ions in the presence of other metal ions Na^+, Mg^{2+}, K^+, Cr^{3+}, Mn^{2+}, Fe^{3+}, Co^{2+}, Ni^{2+}, Cu^{2+}, Zn^{2+}, Cd^{2+}, Hg^{2+} and Pb^{2+}.

4 Conclusions

A novel Schiff base ligand was prepared from 2,6-diformylpyridine and 4-aminoantipyrine and characterized by elemental analysis, FT-IR, ^{1}H-, ^{13}C-NMR and mass spectroscopic studies. Molecular structure of the ligand was determined by single crystal X-ray diffraction study. Sensor ability of the Schiff base ligand to colorimetrically sense metal ions was investigated. Visual colour change of the ligand (0.1mM) was investigated in MeOH solvent in presence of various metal ions (0.1mM), Na^+, Mg^{2+}, Al^{3+}, K^+, Cr^{3+}, Mn^{2+}, Fe^{3+}, Co^{2+}, Ni^{2+}, Cu^{2+}, Zn^{2+}, Cd^{2+}, Hg^{2+} and Pb^{2+}. Upon addition of Al^{3+} ion into the MeOH solution of the ligand, an orange colour developed which is detectable by naked eye.

Supplementary Information

CCDC 975438 contains the supplementary crystallographic data for this paper. These data can be obtained free of charge *via* www.ccdc.cam.ac.uk/data_request/cif, by e-mailingdata_request@ccdc.cam.ac.uk, or by contacting The Cambridge Crystallographic Data Centre 12 Union Road Cambridge CB2 1EZ, UK Fax: +44(0)1223-336033.

References

[1] R.J. Cassella, O.I.B. Magalhaes, M.T. Couto, E.L.S. Lima, M.A.F.S. Neves, F.M.B. Coutinho, Talanta, 67 (2005) 121-128.

[2] S.L.C. Ferreira, A.S. Queiroz, M.S. Fernandes, H.C. dos Santos, Spectrochim. Acta, Part A, 57 (2002) 1939-1950.

[3] M. Arvand, Z. Lashkari, Spectrochim. Acta, Part A, 107 (2013) 280-288.

[4] A.I. Vogel, Textbook of Macro and Semimicro Qualitative Inorganic Analysis, Bungay, New York, 1979, p. 605.

[5] L.W. Potts, Quantitative Analysis. Theory and Practice, Harper and Row, New York, 1987, p. 656.

[6] A. Ali, H. Shen, X. Yin, Analytica Chim. Acta, 369 (1998) 215-223.

[7] D. Kara, A. Fisher**,** Separation & Purification Reviews, 41 (2012) 267-317.

[8] A. Mohadesi, M.A. Taher, Talanta, 72 (2007) 95-100.

[9] A. Mohadesi, M.A. Taher, Talanta, 71 (2007) 615-619.

[10] V.K. Gupta, A.K. Jain, P. Kumar, Sensors and Actuators B: Chemical, 120 (2006) 259-265.

[11] R.N. Goyal, V.K. Gupta, S. Chatterjee, Biosensors and Bioelectronics, 24 (2009) 1649-1654.

[12] V.K. Gupta, A.K. Singh, M.R. Ganjali, P. Norouzi, F. Faridbod, N. Mergu, Sensors and Actuators B: Chemical, 182 (2013) 642-651.

[13] L. Wang, H. Li, D. Cao, Sensors and Actuators B: Chemical, 181 (2013) 749-755.

[14] L.J. Fan, E.J. Wayne, J. Am. Chem. Soc., 128 (2006) 6784-6785.

[15] T. Gunnlaugsson, J.P. Leonard, N.S. Murray, Org. Lett., 6 (2004)1557-1560.

[16] R.S. Sathish, A.G. Raju, G.N. Rao, C. Janardhana, Spec. Chim. Acta Part A: Mol. & Biomol. Spect., 69 (2008) 282-285.

[17] A.J. Blake, N.R. Champness, P. Hubberstey, W.S. Li, M.A. Withersby, M. Schroder, Coor. Chem. Rev., 183 (1999) 117-138.

[18] P.A. Vigato, S. Tamburini, Coor. Chem. Rev., 248 (2004) 1717-2128.

[19] A.Y. Robin, K.M. Fromm, Coor. Chem. Rev., 250 (2006) 2127-2157.

[20] W.M. Singh, B.C. Dash, Pesticides, 22 (1988) 33-37.

[21] O. Bekircan, B. Kahveci, M. Kucuk, Turk. J. Chem., 30 (2006) 29-40.

[22] M.T. Tarafder, A. Kasbollah, N. Saravan, K.A. Crouse, A.M. Ali, O.K. Tin, Biochem., Mol. Bio. & Biophy., 6 (2002) 85-91.

[23] M. Tumer, H. Koksal, M.K. Sener, S. Serin, Trans. Met. Chem., 24 (1999) 414-420.

[24] V.R. Souza, H.R. Rechenberg, J.A. Bonacin, H. Toma, Spec. Chim. Acta Part A: Mol. & Biomol. Spect., 71 (2008) 1296-1301.

[25] L.P. Singh, J.M. Bhatnagar, Talanta, 64 (2004) 313-319.

[26] C.M. Sharaby, Spec. Chim. Acta Part A: Mol. & Biomol. Spect., 66 (2007) 1271-1278.

[27] W. Zhang, J.L. Loebach, S.R. Wilson, E.N. Jacobsen, J. Am. Chem. Soc., 112 (1990) 2801-2803.

[28] S. Radhakrishnan, R. Vijayaragavan, A. Nallamuthu, A. Muthiya, A. Sambandam, V. Sivan, Spec. Chim. Acta Part A: Mol. & Biomol. Spect., 75 (2010) 1146-1151.

[29] R.M.F. Batista, E. Oliveira, S.P.G. Costa, C. Lodeiro, M.M.M. Raposo, Org. Lett., 9 (2007) 3201-3204.

[30] D.F. Wang, Y.C. Ke, H.X. Guo, J. Chen, W. Weng, Spec. Chim. Acta Part A: Mol. & Biomol. Spect., 122 (2014) 268-272.

[31] Bruker APEX2 and SAINT Bruker AXS Inc (1998).

[32] G.M. Sheldrick, A short history of SHELX, Acta Cryst. A, 64 (2008) 112-122.

[33] E.P. Papadopoulos, A. Jarrar, C.H. Issidorides, J. Org. Chem., 31 (1966) 615-616.

[34] S. Menati, A. Azadbakht, R. Azadbakht, A. Taeb, A. Kakanejadifard, Dyes Pigments., 98 (2013) 499-506.

[35] M. Gulcan, H. Zengin, M. Celebi, M. Sonmez, I. Berber, Z. Anorg. Allg. Chem., 639 (2013) 2282-2289.

[36] M.S. Alam, D.U. Lee, J. Chem. Cryst., 42 (2012) 93-102.

[37] G. Ceyhan, M. Tumer, M. Kose, V. McKee, S. Akar, J. Lumin., 132 (2012) 2917-2928.

[38] S. Kim, O.J. Shon, S.H. Yang, J.Y. Kim, M.J. Kim, J. Org. Chem., 67 (2002) 6514-6518.

[39] J.A. Kemlo, T.M. Sheperd, Chem. Phys. Lett., 47 (1977) 158-162.

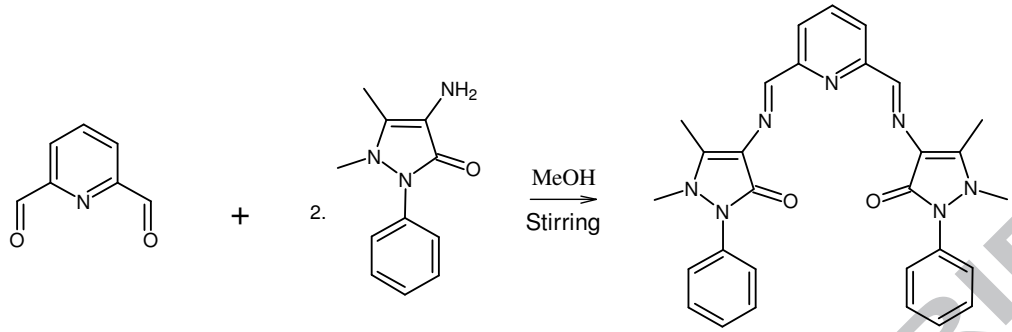

Scheme 1 Preparation of the Schiff base ligand (L).

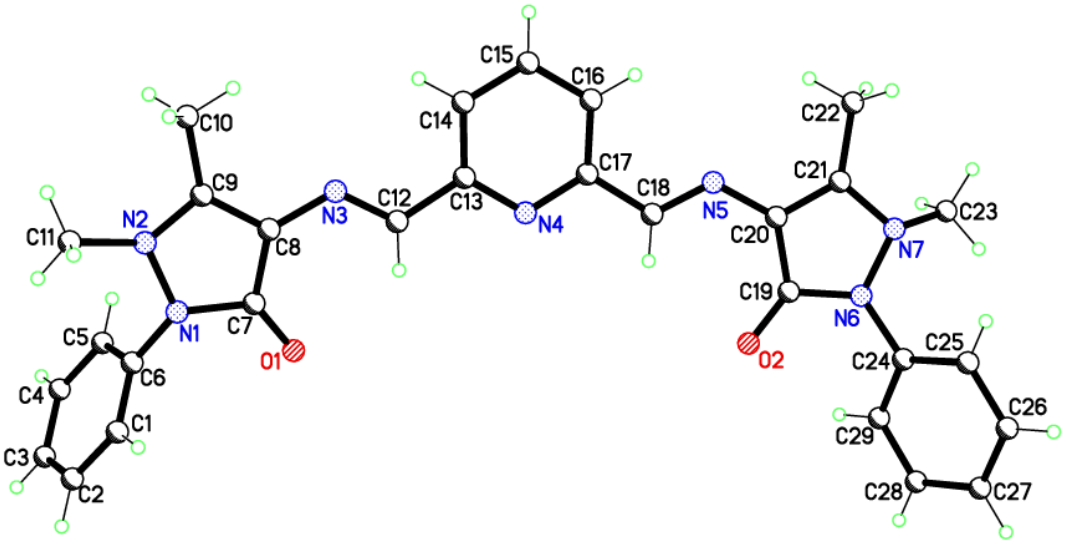

Fig. 1 Perspective view of the ligand with atom numbering.

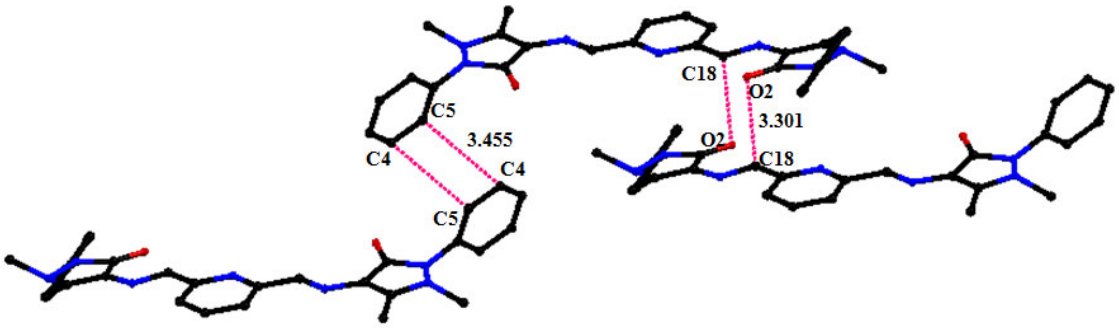

Fig. 2 π...π stacking interactions in the structure.

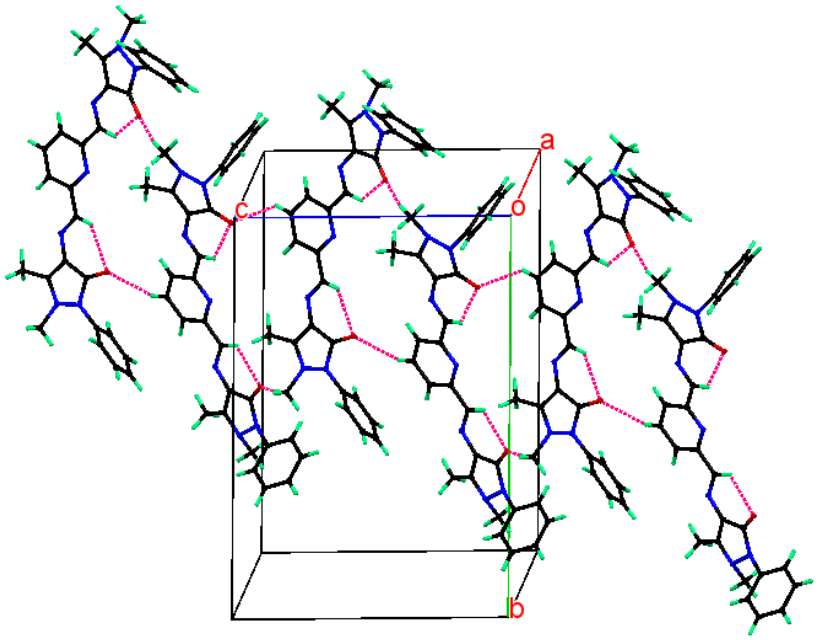

Fig. 3 Hydrogen bond type interactions within the structure.

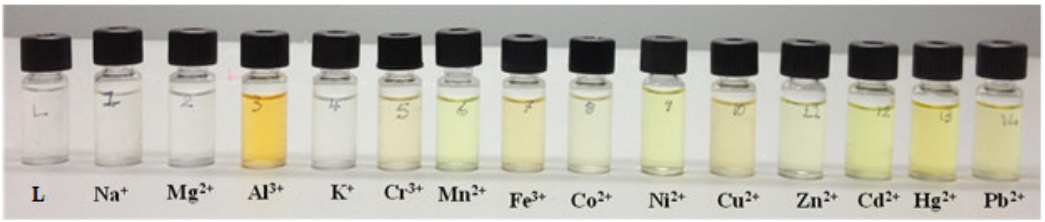

Fig. 4 Colour changes of the ligand (0.1mM) in the presence of various metal ions (0.1 mM) in MeOH in 1:1 (v/v, mL) ratio.

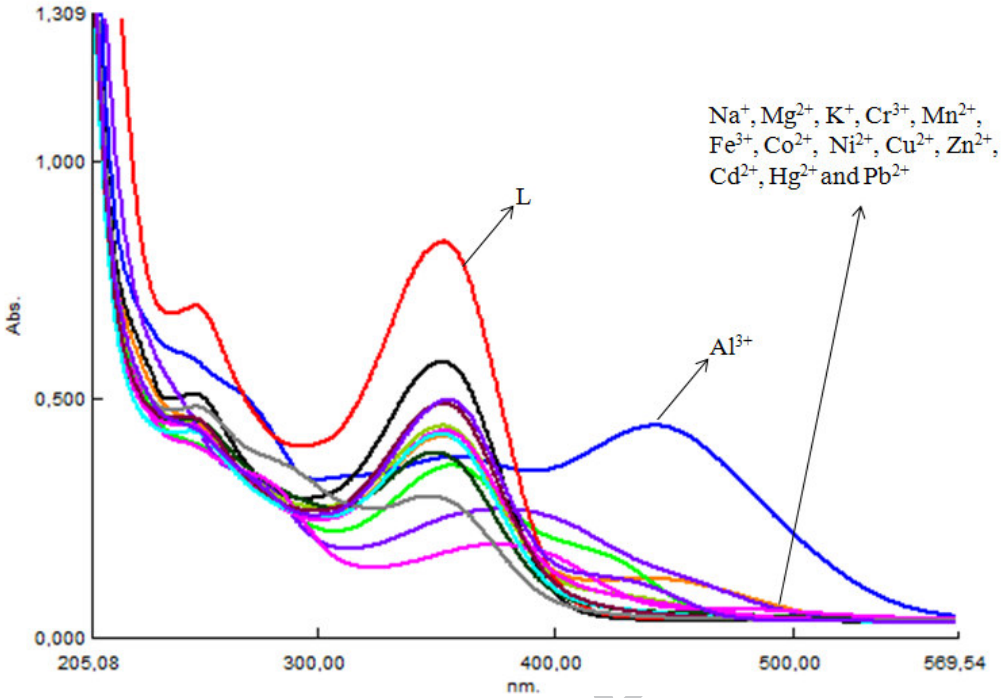

Fig. 5 UV–vis spectral changes of the ligand (0.1 mM) in MeOH upon addition of metal ions in MeOH (0.1 mM) (1:1 (v/v) ratio).

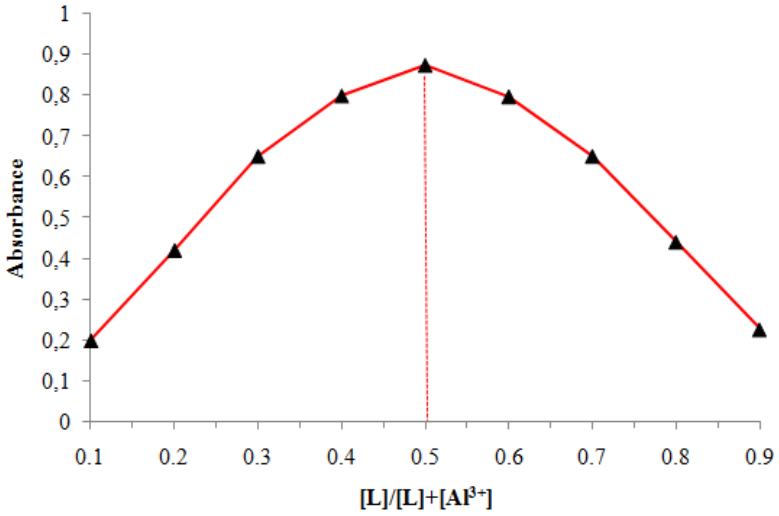

Fig. 6 Job's plot of ligand (L) and $Al^{3+,}$ which indicated 1:1 stoichiometry of ligand-Al^{3+} complex.

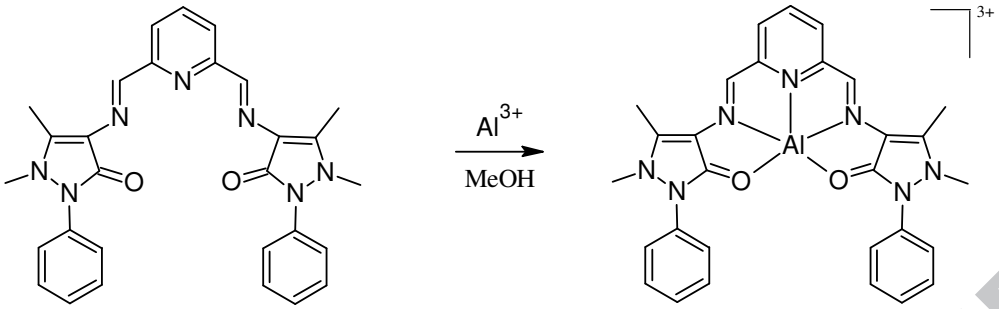

Fig. 7 The possible binding mode of the ligand with Al^{3+}.

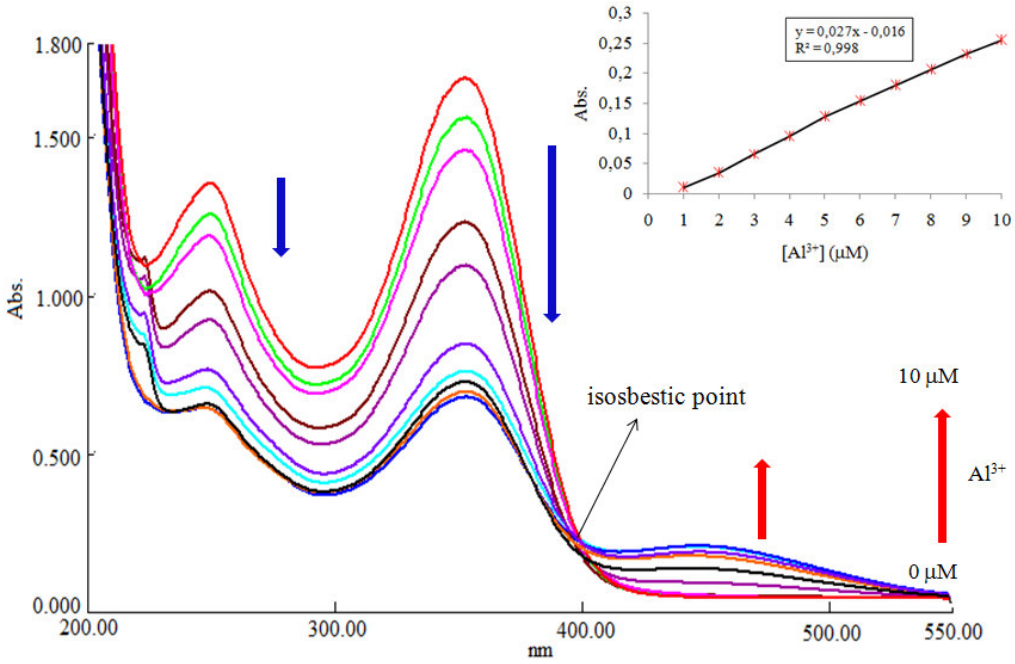

Fig. 8 UV-vis spectra of the ligand with gradual addition of Al^{3+} [1-10 µM, respectively]. Inset: UV-vis absorption intensity at 448 nm vs. concentration of Al^{3+}.

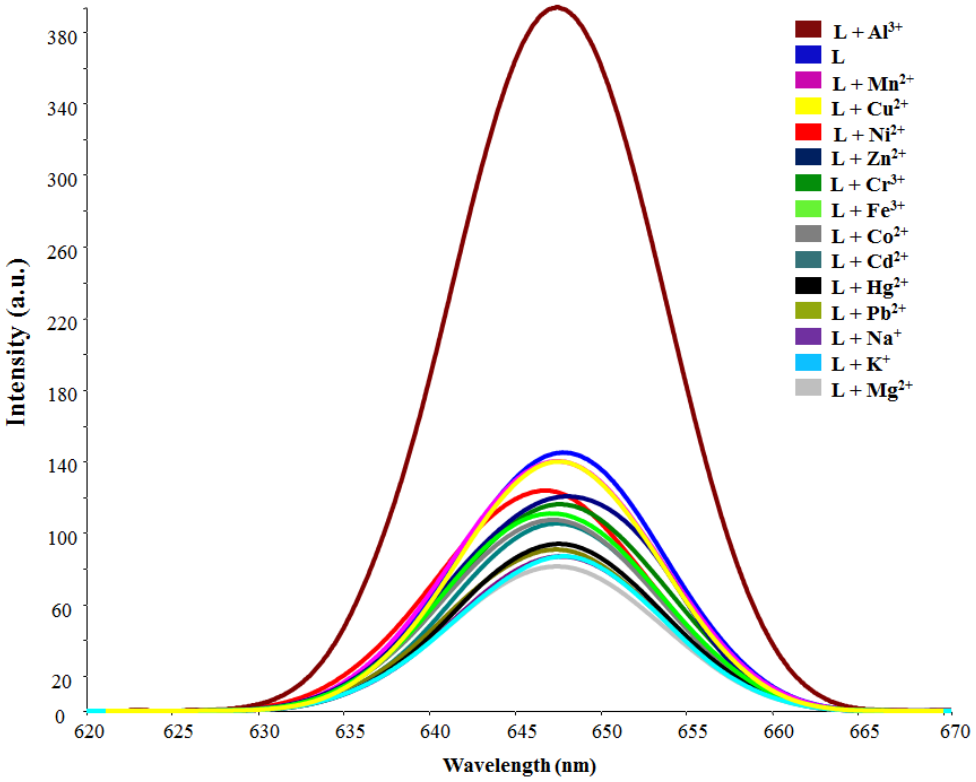

Fig. 9 Fluorescence emission spectra of the ligand (0.1 mM) with different metal ions (0.1mM) in MeOH in 1:1 (v/v, mL) ratio (λ_{em}: 647 nm, λ_{ex}: 560 nm).

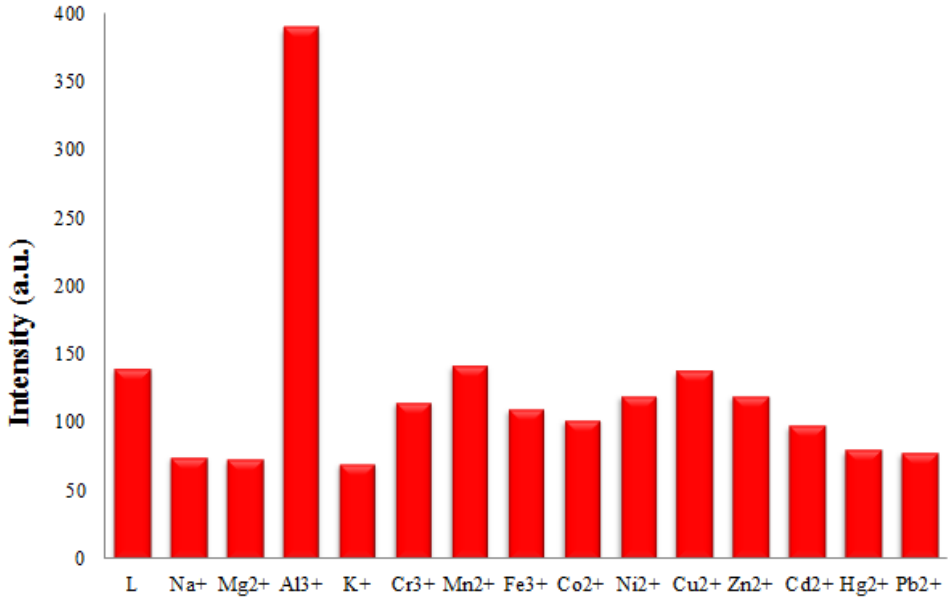

Fig. 10 Fluorescence emission intensity of the ligand (0.1 mM) with different metal ions (0.1 mM) in MeOH in 1:1 (v/v, mL) ratio (λ_{em}: 647 nm, λ_{ex}: 560 nm).

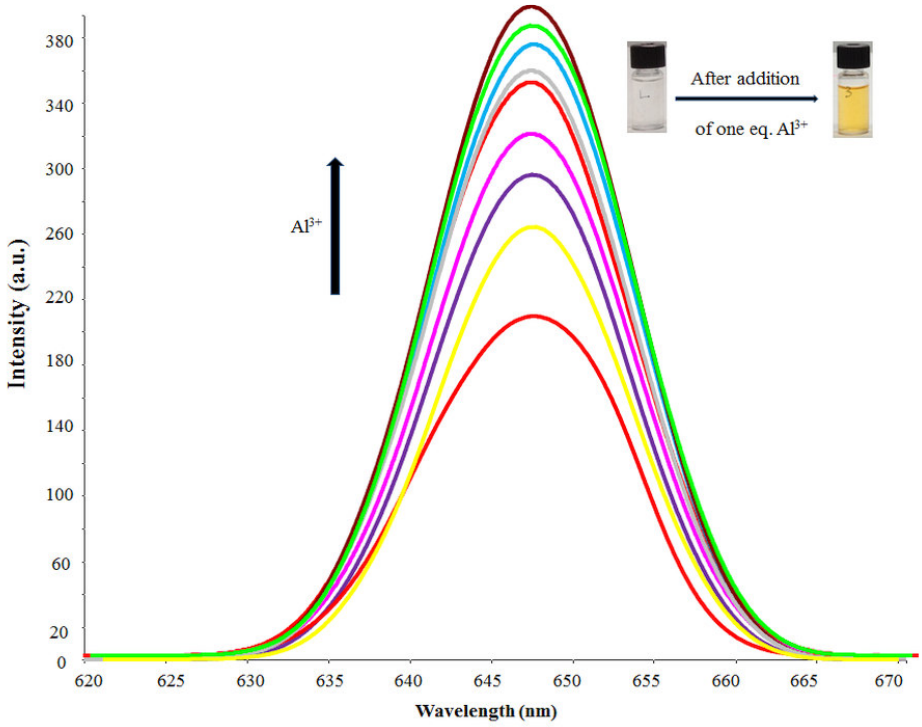

Fig. 11 Fluoroscence emission spectra of the ligand (0.1mM) in MeOH upon addition of Al^{3+}(λ_{em}: 647 nm, λ_{ex}: 560 nm).

Table 1 Crystallographic data for the ligand (L).

Empirical formula		$C_{29}H_{27}N_7O_2$
Formula weight		505.58
Crystal size (mm^3)		0.47 x 0.42 x 0.22
Crystalcolour		colourless
Crystal system		*Monoclinic*
Space group		*P2(1)/n*
Unit cell	*a* (Å)	9.3088(17)
	b (Å)	21.050(4)
	c (Å)	13.575(2)
	α (°)	90
	β (°)	101.424(3)
	γ (°)	90
Volume (Å3)		2607.2(8)
Z		4
Abs. coeff. (mm^{-1})		0.085
Refl. collected		26642
Completeness to θ = 28.02°		99.9 %
Ind. Refl. [R_{int}]		6510 [0.0482]
R1, wR2 [I>2σ (I)]		0.0454, 0.0984
R1, wR2 (all data)		0.0838, 0.1131
CCDC number		975438

Table 2 Selected bond lengths [Å] for the ligand (L).

N(1)-N(2)	1.4084(17)	N(6)-N(7)	1.4140(17)
C(7)-O(1)	1.2362(17)	C(19)-O(2)	1.2354(17)
C(8)-C(9)	1.377(2)	C(20)-C(21)	1.362(2)
N(3)-C(12)	1.2805(17)	C(18)-N(5)	1.2776(18)

Table 3 Hydrogen bonds for the ligand (L) [Å and °].

D-H...A	d(D-H)	d(H...A)	d(D...A)	<(DHA)
C(12)-H(12)...O(1)	0.93	2.49	3.1257(18)	126.0
C(18)-H(18)...O(2)	0.93	2.45	3.0817(18)	125.0
C(15)-H(15)...O(1)*	0.93	2.52	3.239(2)	134.7
C(11)-H(11C)...O(2)*	0.96	2.35	3.292(2)	165.4
C(11)-H(11A)...O(2)**	0.96	2.43	3.347(2)	159.9
C(22)-H(22A)...N(3)***	0.96	2.53	3.342(2)	142.3

Symmetry codes: * x+1/2,-y+1/2, z+1/2 ** -x+1/2, y+1/2, -z+3/2 ***-x+3/2, y-1/2, -z+3/2.

Table 4 Electrochemical data for the ligand (L).

Concentrations	**Scanrate(mV/s)**	E_{pa}**(V)**	E_{pc}**(V)**	***Ipa/Ipc***	$E_{1/2}$**(V)**	ΔE_p**(V)**
1×10^{-3} M	100	-0.13, 0.29, 1.55	1.14, -1.25, -0.65	1.35	-	0.41
	250	-0.11, 0.28, 1.61	0.64, -0.36, -1.28	0.43	-	0.25
	500	-0.40, 0.38, 1.63	0.37, -0.44, -1.31	1.02	0.37	0.82
	750	-0.41, 0.42, 1.71	0.41, -0.40, -1.34	1.02	0.41	0.82
	1000	-0.43,0.48, 1.74	0.38, -0.48, -1.42	0.89	-	0.96
1×10^{-4} M	100	-0.66, 0.17, 1.41	0.61, -0.38, -1.38	1.63	-	0.55
	250	-0.27, 0.24, 1.56	0.59, -0.38, -1.39	0.71	-	0.62
	500	-0.44, 0.33, 1.22	1.38, 0.44, -1.42	0.75		0.98
	750	-0.44, 0.39, 1.18	1.37, 0.29, -1.46	1.34	-	0.10
	1000	-0.41, 0.48, 1.17	1.32, 0.29, -1.52	0.88	-	0.19

All the potentials are referenced to Ag+/AgCl; where *Epa* and *Epc* are anodic and cathodic potentials, respectively. $\Delta Ep = Epa - Epc$. $E1/2 = 0.5 \times (Epa + Ep$

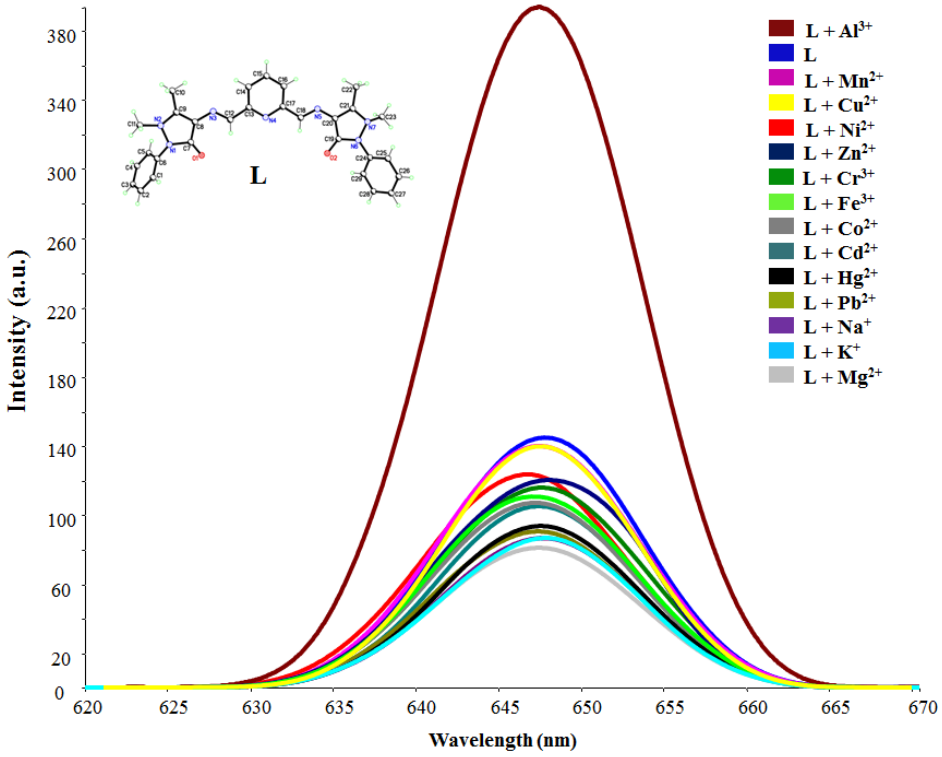

HIGHLIGHTS

- A novel Schiff base compound (L) was synthesised and characterized.
- Molecular structure of the compound was determined by single crystal X-ray diffraction study.
- Visual colour change of the ligand was investigated in MeOH solvent in presence of various metal ions.
- Sensor ability of the Schiff base compound to sense metal ions were investigated by colorimetric and fluorometric methods.